Coherent excitation of a two-state system by a Gaussian field

G. S. Vasilev[1] and N. V. Vitanov[1,2]
[1]*Department of Physics, Sofia University, James Bourchier 5 blvd., 1164 Sofia, Bulgaria*
[2]*Institute of Solid State Physics, Bulgarian Academy of Sciences, Tsarigradsko chaussée 72, 1784 Sofia, Bulgaria*
(Received 3 June 2004; published 16 November 2004)

This work presents an analytic description of the coherent excitation of a two-state quantum system by an external field with a Gaussian temporal shape and a constant frequency. A very accurate analytic approximation to the transition probability is derived by using the Dykhne-Davis-Pechukas approach. This approximation provides analytic expressions for the frequency and amplitude of the probability oscillations, for the excitation profile and excitation linewidth. The linewidth, in particular, shows a weak, logarithmic power broadening.

DOI: 10.1103/PhysRevA.70.053407 PACS number(s): 32.80.Bx, 03.65.Ge, 34.70.+e, 42.50.Vk

I. INTRODUCTION

The two-state quantum system is a fundamental ingredient in quantum mechanics. It can be found in a variety of problems across quantum physics, ranging from nuclear magnetic resonance, coherent atomic excitation, and quantum information to chemical physics, solid-state physics, and neutrino oscillations. Moreover, many problems involving multiple states and complicated linkage patterns can very often be understood only by reduction to one or more two-state problems—e.g., by adiabatic elimination of weakly coupled states [1].

There are several exactly soluble two-state models, including the Rabi [2], Landau-Zener [3], Rosen-Zener [4], Allen-Eberly-Hioe [5], Bambini-Berman [6], Demkov-Kunike [7], Demkov [8], and Nikitin [9] models. Most of these models use various special functions to solve the particular two-state problem. There exist also methods for approximate solutions, such as perturbation theory, the adiabatic approximation, the Magnus approximation, and the Dykhne-Davis-Pechukas approximation.

In the present work, we derive analytically the transition probability for a two-state system driven by a pulsed external field of Gaussian temporal envelope and constant carrier frequency. This field, for which no exact analytic solution is known, is among the most important pulsed fields; e.g., in coherent atomic excitation an ideal phase- and mode-locked pulsed laser delivers Gaussian pulses. We use the Dykhne-Davis-Pechukas (DDP) method [10,11], which involves integration in the complex time plane, to derive a very accurate approximation to the transition probability and the width of the excitation line profile.

The Gaussian pulse shape is somewhat similar to the hyperbolic-secant pulse, for which a beautiful exact analytic solution is known, the Rosen-Zener model [4]. The Gaussian pulse, however, vanishes much faster away from its maximum, which makes it less adiabatic. The comparison between the two shapes reveals interesting pulse-shape effects—e.g., different power broadening.

There are several earlier studies of the Gaussian model. Thomas [12] has shown that the Rosen-Zener conjecture [4] is valid for the Gaussian pulse for very small detunings. Bava *et al.* [13] have found an interesting perturbative solution based on the Rosen-Zener model and valid for small detuning and weak interaction. Berman *et al.* [14] have studied the Gaussian model, along with four other models, and have derived the asymptotic behavior of the transition probability in the limits of small and large values of the ratio of the coupling and detuning. In the present work we extend and generalize these results for arbitrary values of this ratio, which allows us to derive the excitation line shape and linewidth.

This paper is organized as follows. In Sec. II we provide the basic equations and definitions and define the problem. In Sec. III we derive the transition probability by using the DDP method. In Sec. IV, we derive and discuss the linewidth of the excitation profile. We summarize the conclusions in Sec. V.

II. BASIC EQUATIONS AND DEFINITIONS

A. Definition of the problem

Coherent excitation of a two-state quantum system is described by the Schrödinger equation, which in the rotating-wave approximation (RWA) reads [1]

$$i\hbar \frac{d}{dt}\mathbf{c}(t) = \mathsf{H}(t)\mathbf{c}(t), \tag{1}$$

where $\mathbf{c}(t)=[c_1(t),c_2(t)]^T$ is the column vector with the probability amplitudes $c_1(t)$ and $c_2(t)$ of the two states $|\psi_1\rangle$ and $|\psi_2\rangle$, and $\mathsf{H}(t)$ is the Hamiltonian:

$$\mathsf{H}(t) = \hbar \begin{bmatrix} 0 & \frac{1}{2}\Omega(t) \\ \frac{1}{2}\Omega(t) & \Delta \end{bmatrix}. \tag{2}$$

The detuning Δ measures the frequency offset of the field carrier frequency ω from the Bohr transition frequency ω_0, $\Delta=\omega_0-\omega$. The Rabi frequency $\Omega(t)$ quantifies the field-induced coupling between the two states. For example, for laser-atom excitation, $\Omega(t)=-\mathbf{d}\cdot\mathbf{E}(t)/\hbar$, where $\mathbf{d}$ is the atomic transition dipole moment and $\mathbf{E}(t)$ is the laser electric field amplitude.

We are interested in the case when the coupling is a Gaussian pulse and the detuning is constant:

$$\Omega(t) = \Omega_0 e^{-t^2/T^2}, \tag{3a}$$

$$\Delta(t) = \text{const}. \tag{3b}$$

Because the transition probability is an even function of Ω_0, Δ, and T, for simplicity and without loss of generality all these constants will be assumed positive.

If the system is initially in state $|\psi_1\rangle$ $[c_1(-\infty)=1, c_2(-\infty)=0]$, the transition probability after the interaction is given by $\mathcal{P}=|c_2(+\infty)|^2$; its determination is our main concern.

No exact analytic solution to Eq. (1) for the Gaussian model (3) is known. We shall derive below several approximations to $\mathcal{P}$ and calculate from them the period and the amplitude of the probability oscillations, the line shape $\mathcal{P}(\Delta)$, and the linewidth $\Delta_{1/2}$.

B. Adiabatic basis

For the derivation of the transition probability we shall need the adiabatic basis—i.e., the basis of the eigenstates of the Hamiltonian (2). We summarize below the basic definitions and properties of this basis.

In terms of the mixing angle $\vartheta(t)$, defined as

$$\tan 2\vartheta(t) = \frac{\Omega(t)}{\Delta} \quad \left(0 \leqslant \vartheta(t) \leqslant \frac{\pi}{4}\right), \tag{4}$$

the eigenstates of $\mathsf{H}(t)$ read

$$|\varphi_-(t)\rangle = \cos\vartheta(t)|\psi_1\rangle - \sin\vartheta(t)|\psi_2\rangle, \tag{5a}$$

$$|\varphi_+(t)\rangle = \sin\vartheta(t)|\psi_1\rangle + \cos\vartheta(t)|\psi_2\rangle. \tag{5b}$$

The time dependences of the adiabatic states $|\varphi_-(t)\rangle$ and $|\varphi_+(t)\rangle$ derive from the mixing angle $\vartheta(t)$, whereas the bare (diabatic) states $|\psi_1\rangle$ and $|\psi_2\rangle$ are stationary.

Because the Rabi frequency $\Omega(t)$ vanishes at large times and because $\Delta>0$, we have $\vartheta(\pm\infty)=0$; hence,

$$|\varphi_-(\pm\infty)\rangle = |\psi_1\rangle, \tag{6a}$$

$$|\varphi_+(\pm\infty)\rangle = |\psi_2\rangle. \tag{6b}$$

It follows from these relations that a transition between the diabatic states implies a transition between the adiabatic states and vice versa. Hence the transition probability in the adiabatic basis is equal to the transition probability in the diabatic basis.

The energies of the adiabatic states are the eigenvalues of $\mathsf{H}(t)$:

$$\hbar\mathcal{E}_\pm(t) = \frac{\hbar}{2}[\Delta \pm \sqrt{\Omega^2(t)+\Delta^2}]. \tag{7}$$

The splitting between them is given by

$$\hbar\mathcal{E}(t) = \hbar\mathcal{E}_+(t) - \hbar\mathcal{E}_-(t) = \hbar\sqrt{\Omega^2(t)+\Delta^2}. \tag{8}$$

It tends to $\hbar\Delta$ as $t\to\pm\infty$ and its maximum value $\hbar\sqrt{\Omega_0^2+\Delta^2}$ is reached when $\Omega(t)$ is maximal, at $t=0$.

The probability amplitudes in the diabatic and adiabatic bases are connected via the rotation matrix

$$\mathsf{R}(\vartheta) = \begin{bmatrix} \cos\vartheta & \sin\vartheta \\ -\sin\vartheta & \cos\vartheta \end{bmatrix} \tag{9}$$

as

$$\mathbf{c}(t) = \mathsf{R}(\vartheta(t))\mathbf{a}(t), \tag{10}$$

where the column vector $\mathbf{a}(t)=[a_-(t), a_+(t)]^T$ comprises the probability amplitudes of the adiabatic states $|\varphi_-(t)\rangle$ and $|\varphi_+(t)\rangle$. These amplitudes satisfy the transformed Schrödinger equation

$$i\hbar\frac{d}{dt}\mathbf{a}(t) = \mathsf{H}_a(t)\mathbf{a}(t), \tag{11}$$

where the transformed Hamiltonian is given by

$$\begin{aligned}\mathsf{H}_a(t) &= \mathsf{R}^{-1}(\vartheta(t))\mathsf{H}(t)\mathsf{R}(\vartheta(t)) - i\hbar\mathsf{R}^{-1}(\vartheta(t))\dot{\mathsf{R}}(\vartheta(t)) \\ &= \hbar\begin{bmatrix} \mathcal{E}_-(t) & -i\dot\vartheta(t) \\ i\dot\vartheta(t) & \mathcal{E}_+(t) \end{bmatrix},\end{aligned} \tag{12}$$

where the overdots denote time derivatives.

C. Adiabatic condition for the Gaussian model

The condition for adiabatic evolution is

$$|\dot\vartheta| \ll \mathcal{E}(t); \tag{13}$$

i.e., the nonadiabatic coupling in the Hamiltonian (12) must be negligible compared to the eigenenergy splitting. In order to estimate condition (13) for the Gaussian pulse (3) it is convenient to use the adiabaticity function

$$\mathcal{A}(t) = \frac{|\dot\vartheta|}{\mathcal{E}(t)} = \frac{\Omega(t)\Delta\sqrt{\ln[\Omega_0/\Omega(t)]}}{T[\Omega^2(t)+\Delta^2]^{3/2}}. \tag{14}$$

In terms of $\mathcal{A}(t)$ the adiabaticity condition (13) reads $\mathcal{A}(t) \ll 1$. For any fixed Δ, the maximum of this function occurs approximately at $\Omega(t)\sim\Delta/\sqrt{2}$. Hence,

$$\mathcal{A}_{\max} \sim \frac{\sqrt{2\ln(2\Omega_0^2/\Delta^2)}}{3\sqrt{3}\Delta T}. \tag{15}$$

The adiabatic condition can be written as $\mathcal{A}_{\max} < \epsilon$, where ϵ is a small number measuring the deviation from perfect adiabaticity. This leads to the condition

$$\Omega_0 \leqslant \frac{\Delta}{\sqrt{2}}\exp\left(\frac{27}{4}\Delta^2T^2\epsilon^2\right). \tag{16}$$

III. GAUSSIAN MODEL

A. Dykhne-Davis-Pechukas approximation

1. Single transition point

We shall estimate the transition probability $\mathcal{P}$ for the Gaussian model (3) by using the Dykhne-Davis-Pechukas approximation. The DDP formula [10,11] provides the asymptotically exact transition probability between the adia-

batic states in the adiabatic limit. We shall use this formula to calculate the transition probability $\mathcal{P}$ in the original, diabatic basis because, as we discussed above, the transition probabilities in the adiabatic and diabatic bases are equal. The DDP formula reads

$$\mathcal{P} \sim e^{-2\ \mathrm{Im}\ \mathcal{D}(t_0)}, \tag{17}$$

where

$$\mathcal{D}(t_0) = \int_0^{t_0} \mathcal{E}(t)dt. \tag{18}$$

The point t_0 is called the transition point and it is defined as the (complex) zero of the quasienergy splitting,

$$\mathcal{E}(t_0) = 0, \tag{19}$$

which lies in the upper half of the complex t plane (i.e., with $\mathrm{Im}\ t_0 > 0$). Equation (17) gives the correct asymptotic probability for nonadiabatic transitions provided (i) the quasienergy splitting $\mathcal{E}(t)$ does not vanish for real t, including at $\pm\infty$; (ii) $\mathcal{E}(t)$ is analytic and single-valued at least throughout a region of the complex t plane that includes the region from the real axis to the transition point t_0; (iii) the transition point t_0 is well separated from the other quasienergy zero points (if any) and from possible singularities; (iv) there exists a level (or Stokes) line defined by

$$\mathrm{Im}\ \mathcal{D}(t) = \mathrm{Im}\ \mathcal{D}(t_0), \tag{20}$$

which goes from $-\infty$ to $+\infty$ and passes through t_0.

As has been pointed out already by Davis and Pechukas [11], for the Landau-Zener model [3], which possesses a single transition point, the DDP formula (17) gives the exact transition probability, not only in the adiabatic limit, but also in the general case. This amazing feature indicates not only the relevance of the DDP approximation, but raises an intriguing, yet unanswered question: how can an approximate method provide the exact solution?

2. Multiple transition points

In the case of more than one zero point in the upper t plane, Davis and Pechukas [11] have suggested, following George and Lin [15], that Eq. (17) can be generalized to include the contributions from all these N zero points t_k in a coherent sum. This suggestion was later verified by Joye *et al.* [16] and Suominen *et al.* [17–20]. The generalized DDP formula has the form

$$\mathcal{P} \sim \left| \sum_{k=1}^{N} \Gamma(t_k) e^{i\mathcal{D}(t_k)} \right|^2, \tag{21}$$

where $\Gamma(t_k)$ are phase factors defined by

$$\Gamma(t_k) = 4i \lim_{t \to t_k} (t - t_k)\dot{\vartheta}(t). \tag{22}$$

In principle, Eq. (21) should be used when there is more than one transition point lying on the lowest Stokes line (the closest one to the real axis) and should include in principle only the contributions from these points; moreover, Eq. (21) has been rigorously proved only for these transition points [16]. The contributions from the farther zeros are exponentially small and may therefore be neglected. Retaining the contributions from *all* transition points, however, may be beneficial: it has been shown [20] that for the Demkov-Kunike models [7] the full summation in Eq. (21), involving infinitely many transition points, leads to the exact result as for the Landau-Zener model. This is a really astonishing result in view of the fact that the DDP approach is an approximate, perturbative method. For another model, of nonlinear crossing, the contributions from all transition points have been shown to improve the accuracy considerably [21], although there the DDP approximation does not give the exact result. Nevertheless, the validity of Eq. (21) in the general case of arbitrarily many transition points should be considered as an open question.

Another open question for the DDP method is the parameter range where it applies. Strictly, the DDP approximation, being a perturbative result in the adiabatic basis, should be valid only near the adiabatic limit. For a Gaussian field this implies the range defined by the adiabatic condition (16). However, we shall see that the DDP approximation describes very accurately the transition probability well outside this range, virtually for any parameter values, which follows similar earlier successes of this approximation for other models (for some of which, as we discussed, it provides even the exact result). This accuracy of the DDP approximation well beyond the adiabatic regime, essentially in the entire parameter plane, is another open question.

B. Transition points

For the Gaussian model (3), there are infinitely many transition points in the upper half-plane. In terms of the dimensionless time $\tau = t/T = \xi + i\eta$, they are given by

$$\tau_k^{\pm} = \pm \xi_k + i\eta_k, \tag{23a}$$

$$\xi_k = \frac{1}{2}\sqrt{\sqrt{4(\ln\alpha)^2 + (2k+1)^2\pi^2} + 2\ln\alpha}, \tag{23b}$$

$$\eta_k = \frac{1}{2}\sqrt{\sqrt{4(\ln\alpha)^2 + (2k+1)^2\pi^2} - 2\ln\alpha}, \tag{23c}$$

where $k = 0,1,2,\ldots$ and

$$\alpha = \frac{\Omega_0}{\Delta}. \tag{24}$$

The first few pairs of transition points τ_k^- and τ_k^+ are shown in Fig. 1 for three different values of the ratio α. Because $(\xi_k^{\pm})^2 - (\eta_k^{\pm})^2 = \ln\alpha$, for each α the transition points are situated on two symmetric hyperbolas (solid curves in Fig. 1). For $\alpha < 1$ and $\alpha > 1$, the transition points lie on genuine hyperbolas, whereas for $\alpha = 1$ they are on the straight line $\xi_k^{\pm} = \eta_k^{\pm}$. On the other hand, because $\xi_k^{\pm}\eta_k^{\pm} = \pm(2k+1)\pi/4$, the transition points of the same order k lie on another pair of hyperbolas, shown in Fig. 1 by dashed curves.

For $\alpha \ll 1$, we have

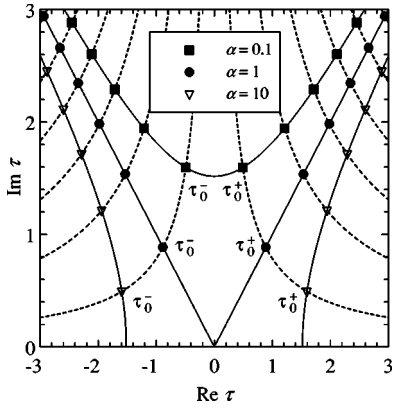

FIG. 1. Transition points for the Gaussian model (3) for three different values of the ratio $\alpha=\Omega_0/\Delta$: 0.1,1,10. The dashed curves show the hyperbolas $\xi\eta=(2k+1)\pi/4$ $(k=0,1,2,\ldots)$ and the solid curves the hyperbolas $\xi^2-\eta^2=\ln\alpha$.

$$\xi_k \sim \frac{(2k+1)\pi}{4\sqrt{\ln(1/\alpha)}} \quad (\alpha \ll 1), \tag{25a}$$

$$\eta_k \sim \sqrt{\ln(1/\alpha)} \quad (\alpha \ll 1). \tag{25b}$$

Hence, as α decreases, the transition points approach the imaginary axis and in the limit $\alpha\to 0$ coalesce (logarithmically) with their counterparts on the other side of the imaginary axis.

For $\alpha \gg 1$, we have

$$\xi_k \sim \sqrt{\ln\alpha} \quad (\alpha \gg 1), \tag{26a}$$

$$\eta_k \sim \frac{(2k+1)\pi}{4\sqrt{\ln\alpha}} \quad (\alpha \gg 1). \tag{26b}$$

As α increases, the transition points approach the real axis and in the limit $\alpha\to\infty$ coalesce (again logarithmically) with the zeros from the lower half-plane (with $\mathrm{Im}\,\tau_k^{\pm}<0$). We shall see that the coalescence of the transition points in the limits $\alpha\to 0$ and $\alpha\to\infty$ do not affect the accuracy of the DDP approximation.

Figure 2 displays the Stokes lines, defined by Eq. (20), emanating from each transition point. Because for the Gaussian model the zeros of the eigenenergy splitting $\mathcal{E}(t)$ are simple and because of the presence of the square root in $\mathcal{E}(t)$, there are three Stokes lines emerging from each transition point [11]. The lowest Stokes line, which connects τ_0^- and τ_0^+ and extends from $-\infty$ to $+\infty$, is the most significant one because it is used in the derivation of the DDP approximation [11] and its existence validates the approximation [16].

C. DDP integrals

Because for the Gaussian model (3) there are infinitely many transition points, the most accurate transition probability is expected to be given by the generalized DDP formula (21). The dominant contributions to the sum in this formula originate from the two transition points closest to the real axis, τ_0^- and τ_0^+. For simplicity, we neglect the contributions

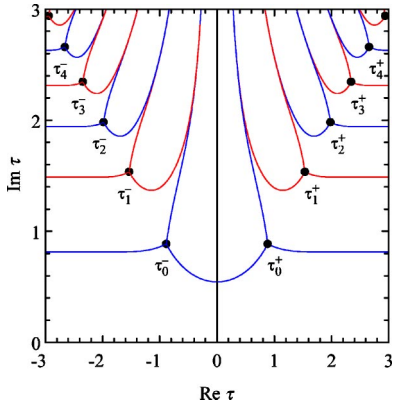

FIG. 2. Numerically calculated Stokes lines for the Gaussian model (3) for $\alpha=\Omega_0/\Delta=1$.

from all others and retain only the terms from these two points.

Because $(\tau_0^-)^*=-\tau_0^+$ and because $\mathcal{E}(\tau)$ is an even function of time, it is easy to show that

$$\mathcal{D}(\tau_0^-) = -\mathcal{D}^*(\tau_0^+), \tag{27}$$

that is, $\mathrm{Re}\,\mathcal{D}(\tau_0^-)=-\mathrm{Re}\,\mathcal{D}(\tau_0^+)$ and $\mathrm{Im}\,\mathcal{D}(\tau_0^-)=\mathrm{Im}\,\mathcal{D}(\tau_0^+)$. Hence it is sufficient to calculate only one of these integrals and we choose $\mathcal{D}(\tau_0^+)$ for this purpose.

Because the imaginary part of the DDP integral $\mathcal{D}(\tau)$ is the same for the two transition points τ_0^+ and τ_0^- [cf. Eq. (27)], these points lie on the same Stokes line, defined by Eq. (20). This Stokes line extends from $-\infty$ to $+\infty$, which is a necessary condition for the validity of the DDP approximation [11,16].

With the arguments presented above, the problem is reduced to the calculation of the DDP integral

$$\mathcal{D}(\tau_0^+) = \Delta T \int_0^{\tau_0^+} \sqrt{\alpha^2 e^{-2\tau^2}+1}\, d\tau. \tag{28}$$

The estimation of this integral will be our main concern hereafter in this section.

1. Behavior of the DDP integral for small α

For small α $(\alpha \ll 1)$ we expand the integrand in Eq. (28) by using the Taylor expansion

$$\sqrt{1+x} = 1 + \sum_{n=1}^{\infty} (-1)^{n-1} \frac{(2n-3)!!}{(2n)!!} x^n, \tag{29}$$

where we assume that $(-1)!!=1$, and perform term-by-term integration. This integration is justified within the circle $|x| \leqq 1$, where the series (29) is uniformly convergent. We choose the path of integration to be the straight line from $\tau=0$ to $\tau=\tau_0^+$ and parametrize this path as $\tau=\tau_0^+ s$ $(0\leqq s\leqq 1)$. It is easy to see that $|\alpha^2 e^{-2\tau^2}| \leqq 1$ along this path. Indeed,

$$|\alpha^2 e^{-2\tau^2}| = \alpha^2 |e^{-2(\tau_0^+)^2 s^2}| = \alpha^{2(1-s^2)} \leqq 1,$$

because $\alpha<1$ and $0\leqq s\leqq 1$.

By using the relation

$$\int_0^{\tau_0^+} e^{-2nu^2} du = \frac{\sqrt{\pi}\,\mathrm{Erf}(\tau_0^+\sqrt{2n})}{2\sqrt{2n}}, \tag{30}$$

we find that

$$\mathcal{D}(\tau_0^+) = \Delta T\left[\tau_0^+ + \sum_{n=1}^{\infty}(-1)^{n-1}\frac{(2n-3)!!}{(2n)!!} \times \frac{\alpha^{2n}\sqrt{\pi}\,\mathrm{Erf}(\tau_0^+\sqrt{2n})}{2\sqrt{2n}}\right], \tag{31}$$

where $\mathrm{Erf}(x)$ is the error function [22]. Using Eqs. (25), we find the dominant asymptotic terms as

$$\mathrm{Re}\,\mathcal{D}(\tau_0^+) \sim \frac{\pi\Delta T}{4\sqrt{\ln(1/\alpha)}} \quad (\alpha \ll 1), \tag{32a}$$

$$\mathrm{Im}\,\mathcal{D}(\tau_0^+) \sim \Delta T\sqrt{\ln(1/\alpha)} \quad (\alpha \ll 1). \tag{32b}$$

2. Behavior of the DDP integral for large α

Calculation by power series expansion. For large α ($\alpha \gg 1$) we write the integral (28) as

$$\mathcal{D}(\tau_0^+) = \Delta T\int_0^{\tau_0^+} \alpha e^{-\tau^2}\sqrt{1+\alpha^{-2}e^{2\tau^2}}\,d\tau. \tag{33}$$

Again, as for $\alpha \ll 1$, we choose the straight line from $\tau=0$ to $\tau=\tau_0^+$ as the integration path and parametrize it as $\tau=\tau_0^+ s$ ($0 \leqq s \leqq 1$). Since $|\alpha^{-2}e^{2\tau^2}| = \alpha^{-2(1-s^2)} \leqq 1$ (due to $\alpha > 1$ and $0 \leqq s \leqq 1$), we can again use the expansion (29) and term-by-term integration to find

$$\mathcal{D}(\tau_0^+) = \frac{\sqrt{\pi}}{2}\Omega_0 T\left[\mathrm{Erf}(\tau_0^+) + i\sum_{n=1}^{\infty}(-1)^n\frac{(2n-3)!!}{(2n)!!} \times \frac{\alpha^{-2n}\mathrm{Erf}(i\tau_0^+\sqrt{2n-1})}{\sqrt{2n-1}}\right]. \tag{34}$$

The dominant asymptotic terms are

$$\mathrm{Re}\,\mathcal{D}(\tau_0^+) \sim \frac{\sqrt{\pi}}{2}\Omega_0 T \quad (\alpha \gg 1), \tag{35a}$$

$$\mathrm{Im}\,\mathcal{D}(\tau_0^+) \sim \frac{\pi\Delta T}{4\sqrt{\ln\alpha}} \quad (\alpha \gg 1), \tag{35b}$$

where for the real part we have used the asymptotics of the error function [22], $\mathrm{Erf}(z) \sim 1$ ($|z| \to \infty, |\arg z| < 3\pi/4$), whereas for the imaginary part we have used Eq. (A1) in the Appendix.

Calculation by the method of steepest descent. We now apply the method of steepest descent [23] to calculate the integral (28). We represent the integral as

$$W = \int_C e^{-F(\tau)}d\tau, \tag{36}$$

where $F(\tau) = -\ln\sqrt{\alpha^2 e^{-2\tau^2}+1}$ and the contour C is a curve connecting 0 and τ_0^+. The saddle point, defined by $F'(\tau_s)=0$, is $\tau_s=0$. The integral has the asymptotics [23]

$$W \sim \sqrt{\frac{\pi}{2F_2}}e^{-F_0}[Q_0 + Q_2 + \cdots], \tag{37}$$

provided $|\arg F_2| < \pi$, where $Q_0=1$, $Q_2=5F_3^2-3F_2F_4$, etc., with $F_n = F^{(n)}(\tau_s)$. We find $F_0 = -\ln\sqrt{\alpha^2+1}$, $F_2 = 2\alpha^2/(\alpha^2+1)$, etc. Hence for large α the dominant term is

$$\mathcal{D}(\tau_0^+) \sim \frac{\sqrt{\pi}}{2}\Delta T\frac{\alpha^2+1}{\alpha} \sim \frac{\sqrt{\pi}}{2}\Omega_0 T. \tag{38}$$

This result coincides with Eq. (35a).

Because the saddle point $\tau_s=0$ is real and the function $F(\tau)$ and all of its derivatives are real in this point, the method of steepest descent provides only the real part of the integral (28). Moreover, this method can deliver only the large-α asymptotics because the expansion (37) is in terms of the inverse powers of α.

We derive below, using a middle-point method, uniform approximations to $\mathrm{Re}\,\mathcal{D}(\tau_0^+)$ and $\mathrm{Im}\,\mathcal{D}(\tau_0^+)$, valid for any value of α.

3. Uniform approximation to the DDP integral

We shall derive a uniform approximation to the DDP integral $\mathcal{D}(\tau_0^+)$, Eq. (28), by choosing an appropriate integration contour. We require on this contour the integrand $f(\tau)$ to be real, where

$$f(\tau) = \sqrt{\alpha^2 e^{-2\tau^2}+1} = \sqrt{\alpha^2 e^{2(\eta^2-\xi^2)-4i\xi\eta}+1}. \tag{39}$$

Then the complexity will originate solely from the integration path, which greatly facilitates the derivation of the real and imaginary parts of the integral. $\mathrm{Im}\,f^2(\tau)$ vanishes when

$$4\xi\eta = k\pi \quad (k = 0, \pm1, \pm2, \ldots). \tag{40}$$

The latter equation defines a family of hyperbolas (for $k=0$ the corresponding hyperbola degenerates into the axes $\xi=0$ and $\eta=0$). The initial point $\tau=0$ of the integration path obviously lies on the $k=0$ hyperbola. The final point of the integration path τ_0^+ lies on the hyperbola with $k=1$ in the first quadrant. Hence we can connect the initial and final points of the integration path by first going from the origin to infinity along the real axis (staying on the $k=0$ hyperbola) and then returning to the transition point τ_0^+ along the $k=1$ hyperbola $4\xi\eta=\pi$. This integration path is drawn in Fig. 3. On this path the integrand $f(\tau)$ is always real. [Had we approached τ_0^+ on the $k=1$ hyperbola from above, from $i\infty$, then $f(\tau)$ would be imaginary.]

We shall first calculate $\mathrm{Im}\,\mathcal{D}(\tau_0^+)$, which is simpler, and then $\mathrm{Re}\,\mathcal{D}(\tau_0^+)$.

Imaginary part of the DDP integral. For the imaginary part of the DDP integral (28) we have

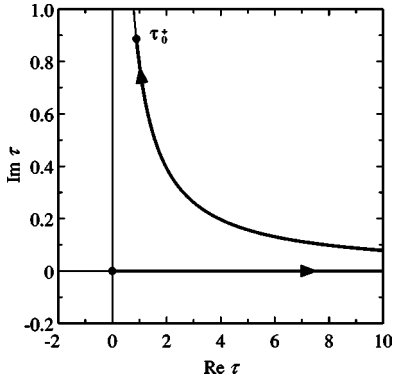

FIG. 3. Integration contour for the calculation of the integral $\mathcal{D}(\tau_0^+)$ for $\alpha=1$.

$$\begin{aligned}\mathrm{Im}\,\mathcal{D}(\tau_0^+) &= \Delta T\,\mathrm{Im}\left(\int_0^{+\infty} + \int_{+\infty}^{\tau_0^+}\right) f(\tau)d\tau \\ &= \Delta T\,\mathrm{Im}\int_0^{\eta_0} g(\eta)\left(-\frac{\pi}{4\eta^2}+i\right)d\eta \\ &= \Delta T\int_0^{\eta_0} g(\eta)d\eta, \end{aligned} \tag{41}$$

with

$$g(\eta)=\sqrt{1-\alpha^2 e^{2\pi^2-\pi^2/8\eta^2}}, \tag{42}$$

where we have used that the integral on the real axis part $[0,+\infty)$ is real and we have changed the integration variable in the second integral from τ to η through $\tau=\pi/4\eta+i\eta$ (since $\xi=\pi/4\eta$ on the $k=1$ hyperbola).

The integrand $g(\eta)$ is a monotonically decreasing function of η, which has its maximum at $\eta=0, g_{\max}=g(0)=1$, as shown in Fig. 4. This provides a justification for approximating the integral by replacing the integrand $g(\eta)$ by its maximum value $g_{\max}$ and in return shrinking the integration interval from $[0,\eta_0]$ to $[0,\eta_\lambda]$ where η_λ is a free parameter for the moment. An argument in support of this approximation is that the error from the neglected contribution from the interval $[\eta_\lambda,\eta_0]$ (region B) can be compensated by the error from

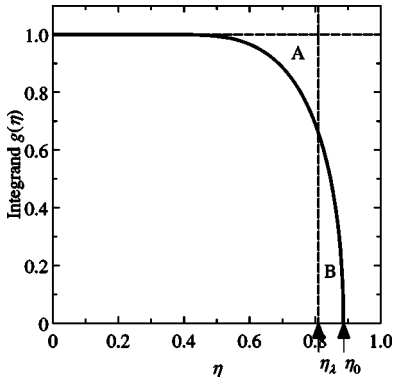

FIG. 4. Integrand $g(\eta)$ of the integral $\mathrm{Im}\,\mathcal{D}(\tau_0^+)$, Eq. (41).

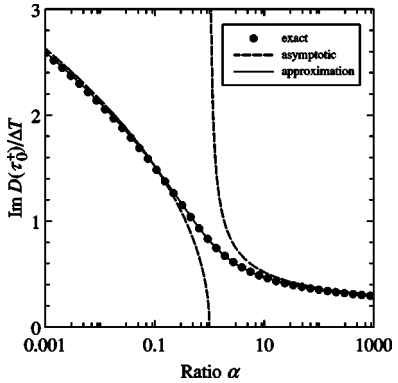

FIG. 5. The imaginary part of the DDP integral $\mathrm{Im}\,\mathcal{D}(\tau_0^+)$ versus the ratio parameter $\alpha=\Omega_0/\Delta$. The dots show the exact numeric values, the solid curve the uniform approximation (44), and the dashed curves the asymptotic formulas (32b) and (35b) for small and large α, respectively.

the overestimation of the function $g(\eta)$ by its maximum $g_{\max}=1$ in the interval $[0,\eta_\lambda]$ (region A).

We choose η_λ to be the point at which $g(\eta)$ decreases to $\lambda g_{\max}$, where the number λ remains to be fixed. We find from here that

$$\eta_\lambda=\frac{1}{2}\sqrt{\sqrt{4\ln^2(m\alpha)+\pi^2}-2\ln(m\alpha)}, \tag{43}$$

where $m=1/\sqrt{1-\lambda^2}$. Then the integral (41) is approximated as $\mathrm{Im}\,\mathcal{D}(\tau_0^+)\approx\Delta T g_{\max}\eta_\lambda$—i.e.,

$$\mathrm{Im}\,\mathcal{D}(\tau_0^+)\approx\frac{1}{2}\Delta T\sqrt{\sqrt{4\ln^2(m\alpha)+\pi^2}-2\ln(m\alpha)}. \tag{44}$$

Obviously, for each α, both η_λ or λ can be chosen such that Eq. (44) provides the exact result; then, however, η_λ and λ will be functions of α and this calculation is equivalent to solving the integral. We fix the value of λ by requesting Eq. (44) to provide the exact result for $\alpha=1$; this gives $\lambda\approx0.646\,983$ and $m\approx1.311\,468$.

The advantage of this choice is that the approximation (44), besides providing the exact result for $\alpha=1$ (i.e., $\Omega_0=\Delta$), is also very accurate in some vicinity of this important point. On the other hand, Eq. (44) has the following asymptotics:

$$\mathrm{Im}\,\mathcal{D}(\tau_0^+)\sim\Delta T\sqrt{\ln(m/\alpha)}\quad(\alpha\ll1), \tag{45a}$$

$$\mathrm{Im}\,\mathcal{D}(\tau_0^+)\sim\frac{\pi\Delta T}{4\sqrt{\ln(m\alpha)}}\quad(\alpha\gg1). \tag{45b}$$

These expressions agree with Eqs. (32b) and (35b), except for the factor m, which is insignificant in the limits $\alpha\gg1$ and $\alpha\ll1$ [since $\ln(m\alpha)=\ln m+\ln\alpha\approx\ln\alpha$ for $\alpha\gg1$ and similarly for $\alpha\ll1$]. This factor becomes significant for intermediate α, where, however, the accuracy of Eq. (44) improves until, as explained above, it becomes exact for $\alpha=1$.

Figure 5 shows $\mathrm{Im}\,\mathcal{D}(\tau_0^+)$ plotted versus the ratio parameter α. The analytic approximation (44) is undistinguishable from the exact result. The asymptotic formulas (32b) and

(35b) describe the asymptotic behaviors for small and large α very accurately.

Real part of the DDP integral. For the real part of the DDP integral (28) we follow the same path of integration as for the imaginary part, Fig. 3. We have

$$\begin{aligned}\mathrm{Re}\,\mathcal{D}(\tau_0^+) &= \Delta T\,\mathrm{Re}\left(\int_0^{+\infty} + \int_{+\infty}^{\tau_0^+}\right) f(\tau)d\tau \\ &= \Delta T\left[\int_0^{+\infty} f(\tau)d\tau - \int_{\xi_0}^{+\infty} h(\xi)d\xi\right] \\ &= \Delta T[\mathcal{I}_1(\alpha) + \mathcal{I}_2(\alpha) + \xi_0(\alpha)],\end{aligned} \tag{46}$$

where $f(\tau)$ is defined by Eq. (39), $h(\xi)$ by

$$h(\xi) = \sqrt{1 - \alpha^2 e^{-2\xi^2 + \pi^2/8\xi^2}}, \tag{47}$$

and

$$\mathcal{I}_1(\alpha) = \int_0^{+\infty} [f(\tau) - 1]d\tau, \tag{48a}$$

$$\mathcal{I}_2(\alpha) = \int_{\xi_0}^{+\infty} [1 - h(\xi)]d\xi. \tag{48b}$$

Here we have first changed the integration variable in the latter integral from τ to ξ by the substitution $\tau = \xi + i\pi/4\xi$ (since $\eta = \pi/4\xi$ on the $k=1$ hyperbola) in order to replace the complex contour integral by a real one. Then we have added and substracted the term 1 in order to make both integrals convergent.

We shall estimate $\mathcal{I}_1(\alpha)$ and $\mathcal{I}_2(\alpha)$ by using the midpoint method used above for $\mathrm{Im}\,\mathcal{D}(\tau_0^+)$. We begin with the integral $\mathcal{I}_1(\alpha)$. The integrand has its maximum value $\sqrt{\alpha^2+1}-1$ at $\tau=0$ and decreases monotonically as τ increases. We introduce the number τ_ν as the value of τ at which the integrand decreases to ν times of its maximum. From here we find

$$\tau_\nu = \sqrt{\frac{1}{2}\ln\frac{\alpha^2}{[1 + \nu(\sqrt{\alpha^2+1} - 1)]^2 - 1}}. \tag{49}$$

The integral $\mathcal{I}_1(\alpha)$ is approximated as

$$\mathcal{I}_1(\alpha) \approx (\sqrt{\alpha^2+1} - 1)\tau_\nu. \tag{50}$$

By requesting that this approximation give the exact value of $\mathcal{I}_1(\alpha)$ for $\alpha=1$ we find $\nu = 0.462\,350\ldots$.

We now turn to the calculation of the second integral $\mathcal{I}_2(\alpha)$. Again its integrand is a monotonically decreasing function of the argument ξ with a maximum equal to 1 in the beginning ξ_0 of the integration interval [there $h(\xi)=0$]. We introduce the number ξ_μ as the value of ξ at which the integrand decreases to μ times of its maximum. From here,

$$\xi_\mu = \frac{1}{2}\sqrt{\sqrt{\left[\ln\frac{\alpha^2}{\mu(2-\mu)}\right]^2 + \pi^2} + \ln\frac{\alpha^2}{\mu(2-\mu)}}. \tag{51}$$

The integral $\mathcal{I}_2(\alpha)$ is approximated as

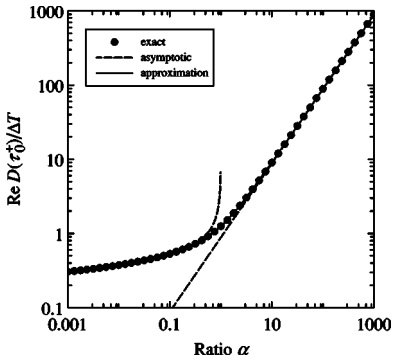

FIG. 6. The real part of the DDP integral $\mathrm{Re}\,\mathcal{D}(\tau_0^+)$ versus the ratio parameter $\alpha=\Omega_0/\Delta$. The dots show the exact numeric result, the solid curve the uniform approximation (53), and the dashed curves the asymptotic formulas (32a) and (35a) for small and large α, respectively.

$$\mathcal{I}_2(\alpha) \approx \xi_\mu(\alpha) - \xi_0(\alpha). \tag{52}$$

By requesting that this approximation give the exact value of $\mathcal{I}_2(\alpha)$ for $\alpha=1$, we find $\mu = 0.316\,193\ldots$ and $\mu(2-\mu) = 0.532\,408\ldots$.

Combining the results in this section, we find

$$\begin{aligned}\mathrm{Re}\,\mathcal{D}(\tau_0^+) \approx \Delta T\Bigg\{ &(\sqrt{\alpha^2+1} - 1) \\ &\times\sqrt{\frac{1}{2}\ln\frac{\alpha^2}{[1 + \nu(\sqrt{\alpha^2+1} - 1)]^2 - 1}} \\ &+ \frac{1}{2}\sqrt{\sqrt{\left[\ln\frac{\alpha^2}{\mu(2-\mu)}\right]^2 + \pi^2} + \ln\frac{\alpha^2}{\mu(2-\mu)}}\Bigg\}.\end{aligned} \tag{53}$$

For $\alpha=1$, Eq. (53) gives the exact result. In the limit of small α, the second term dominates and Eq. (53) gives

$$\mathrm{Re}\,\mathcal{D}(\tau_0^+) \sim \frac{\pi\Delta T}{4\sqrt{\ln(1/\alpha)}} \quad (\alpha \ll 1), \tag{54}$$

which is the same as the correct asymptotics (32a). For large α, it is the first term in Eq. (53) that dominates and $\mathrm{Re}\,\mathcal{D}(\tau_0^+)$ reduces to

$$\mathrm{Re}\,\mathcal{D}(\tau_0^+) \sim \Omega_0 T\sqrt{\ln\frac{1}{\nu}} \quad (\alpha \gg 1). \tag{55}$$

This result is slightly different (in the numeric factor) from the correct asymptotics (35a) for large α. However, this difference is less than 1% because $\sqrt{\ln(1/\nu)} \approx 0.878$ in Eq. (55), compared to $\sqrt{\pi}/2 \approx 0.886$ in Eq. (35a).

Figure 6 shows $\mathrm{Re}\,\mathcal{D}(\tau_0^+)$ plotted versus the ratio parameter α. The analytic approximation (53) virtually coincides with the exact values. The asymptotic formulas (32a) and (35a) describe accurately the asymptotic behaviors for small and large α.

4. Comparison with earlier work

The results in the present paper are related to earlier results by Berman and co-workers [14], who have studied the Gaussian model, along with four other models, and have derived the asymptotic behaviors of the DDP integral $\mathcal{D}(\tau_0^+)$. The asymptotic behaviors of Re $\mathcal{D}(\tau_0^+)$ found here, Eqs. (32a) and (35a), are the same as the results in Ref. [14]. The asymptotics of Im $\mathcal{D}(\tau_0^+)$ for small α, Eq. (32b), also coincides with the result of Ref. [14]. The asymptotic behavior of Im $\mathcal{D}(\tau_0^+)$ for large α, however, differs. Indeed, the result [Eq. (38e)] of Ref. [14],

$$\mathrm{Im}\,\mathcal{D}(\tau_0^+) \sim \frac{\pi \Delta T}{4\ln\sqrt{\alpha}} \quad (\alpha \gg 1), \tag{56}$$

differs significantly from Eq. (35b). As Fig. 5 shows, our result (35b) provides the correct asymptotic behavior for large α. We have verified that Eq. (56) deviates considerably from the exact result.

D. Transition probability

1. Transition probability

In order to sum the contributions from various DDP integrals we need the factors Γ_k, Eq. (22). One finds after simple algebra that

$$\Gamma(\tau_k^{\pm}) = \pm(-1)^k. \tag{57}$$

Now we have all the ingredients to calculate the transition probability $\mathcal{P}$. Collecting the results from Eqs. (21), (44), (53), and (57), we find

$$\mathcal{P} \sim 4\exp[-2\,\mathrm{Im}\,D(\tau_0^+)]\sin^2[\mathrm{Re}\,\mathcal{D}(\tau_0^+)]. \tag{58}$$

We replace this expression by

$$\mathcal{P} \sim \frac{\sin^2[\mathrm{Re}\,\mathcal{D}(\tau_0^+)]}{\cosh^2[\mathrm{Im}\,\mathcal{D}(\tau_0^+)]}. \tag{59}$$

There are several arguments in favor of this replacement. First of all, the error we make when replacing Eq. (58) with Eq. (59) is comparable or smaller, and therefore negligible, compared to the errors in neglecting the higher-order terms in the calculation of the DDP integral (28), the errors from the neglect of the higher transition points $\tau_k^{\pm}$ ($k \geqslant 1$), and the DDP approximation itself. Second, Eq. (59) is superior to Eq. (58) because it does not violate unitarity ($\mathcal{P} \leqslant 1$), whereas Eq. (58) does (albeit only outside its range of validity). Third, such a replacement has already been used [24] and shown to improve the accuracy. Last, such a replacement in $\mathcal{P}$ of an exponent by a hyperbolic secant occurs in the Rosen-Zener model, which is similar in many respects to the Gaussian model (3), when adding the contributions from all transition points [20]. This is particularly important in view of the fact that such a summation provides the exact transition probability in the Rosen-Zener model.

There is an additional, even more convincing argument supporting the replacement of Eq. (58) by Eq. (59): in the limit $\alpha \gg 1$ this replacement can be proved rigorously. Indeed, for $\alpha \gg 1$ the real and imaginary parts of the DDP integrals $\mathcal{D}(\tau_k^+)$ have the behaviors

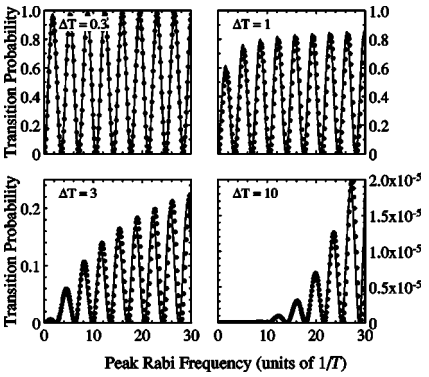

FIG. 7. Transition probability for the Gaussian pulse plotted vs the peak Rabi frequency Ω_0 for four values of the detuning, $\Delta T = 0.3, 1, 3, 10$. The exact results obtained by numerical integration of the Schrödinger equation are shown by dots and our approximation, Eqs. (59), (44), and (53), by solid lines.

$$\mathrm{Re}\,\mathcal{D}(\tau_k^+) \sim \mathrm{Re}\,\mathcal{D}(\tau_0^+), \tag{60a}$$

$$\mathrm{Im}\,\mathcal{D}(\tau_k^+) \sim (2k+1)\mathrm{Im}\,\mathcal{D}(\tau_0^+). \tag{60b}$$

The asymtpotics of Re $\mathcal{D}(\tau_k^+)$ can be derived in the same manner as Eq. (35a), whereas the asymptotics of Im $\mathcal{D}(\tau_k^+)$ is derived in the Appendix, Eq. (A1). With the phase factors (57) included the generalized DDP formula (21) reads

$$\mathcal{P} \sim 4\left[\sum_{k=0}^{\infty}(-1)^k e^{-(2k+1)\mathrm{Im}\,\mathcal{D}(\tau_0^+)}\right]^2 \sin^2[\mathrm{Re}\,D(\tau_0^+)], \tag{61}$$

which leads immediately to Eq. (59).

2. Examples

Equation (59) with the approximations (53) and (44) for Re $\mathcal{D}(\tau_0^+)$ and Im $\mathcal{D}(\tau_0^+)$ provides a very accurate description of the transition probability $\mathcal{P}$. The latter is plotted on Fig. 7 as a function of the peak Rabi frequency Ω_0 for four different values of the detuning Δ. As Ω_0 increases, Rabi-like oscillations are observed, with both amplitude and frequency matched very well by our approximation (59).

In Fig. 8 the transition probability $\mathcal{P}$ is plotted versus the detuning Δ for four different values of the peak Rabi frequency Ω_0. Both the line shape and linewidth are described very accurately by our approximation (59). Note that the linewidth increases only marginally as $\Omega_0 T$ increases from 5 to 200, indicating a very weak power broadening; we shall return to this observation in Sec. IV.

3. Comparison of the Gaussian model and the Rosen-Zener model

It is interesting to compare the Gaussian model with the exactly soluble Rosen-Zener (RZ) model [4]. In the RZ model, the Rabi frequency has a hyperbolic-secant shape and the detuning is constant:

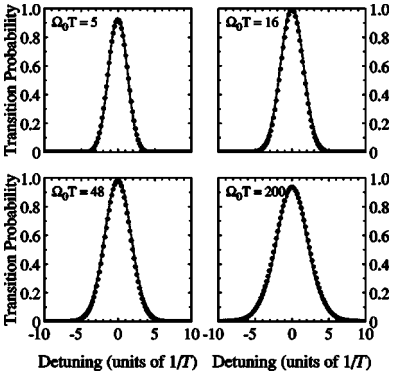

FIG. 8. Transition probability for the Gaussian pulse plotted vs the detuning Δ for four values of the peak Rabi frequency, $\Omega_0 T = 5,16,48,200$. The exact results obtained by numerical integration of the Schrödinger equation are shown by dots and our approximation (59) by solid lines.

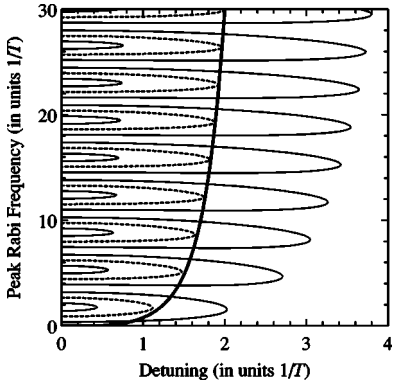

FIG. 9. The transition probability for the Gaussian pulse as a function of the detuning Δ and the peak Rabi frequency Ω_0. The three sets of concentric curves show the level lines of transition probabilities 0.9 (inner), 0.5 (dashed), and 0.1 (outer). The thick curve illustrates the analytic linewidth calculated from Eq. (64).

$$\Omega(t) = \Omega_0 \,\mathrm{sech}(t/T), \tag{62a}$$

$$\Delta(t) = \mathrm{const}. \tag{62b}$$

The sech shape is very similar to the Gaussian shape, but its wings vanish more slowly; that is, the sech pulse is more adiabatic. The transition probability for the RZ model is given exactly by

$$\mathcal{P} = \frac{\sin^2\left(\frac{1}{2}\pi\Omega_0 T\right)}{\cosh^2\left(\frac{1}{2}\pi\Delta T\right)}. \tag{63}$$

In this model, the dependence of $\mathcal{P}$ on the Rabi frequency and the detuning factorizes, which is a unique feature. The oscillation amplitude is determined solely by the detuning Δ and the phase of the oscillations depends only on the peak Rabi frequency Ω_0.

For the Gaussian pulse, the oscillation phase $\mathrm{Re}\,\mathcal{D}(\tau_0^+)$, Eq. (53), depends both on Ω_0 and Δ. For $\Omega_0 \ll \Delta$, $\mathrm{Re}\,\mathcal{D}(\tau_0^+)$ depends primarily on Δ and only logarithmically on Ω_0 [see Eq. (54)]. In contrast, for $\Omega_0 \gg \Delta$, $\mathrm{Re}\,\mathcal{D}(\tau_0^+)$ is determined by Ω_0 [cf. Eq. (55)], as in the RZ model.

The oscillation amplitude $\mathrm{sech}^2[\mathrm{Im}\,\mathcal{D}(\tau_0^+)]$ in the Gaussian model, Eq. (44), depends, for all ratios of Ω_0 and Δ, primarily on Δ, as in the RZ model. In contrast to the RZ model, however, this amplitude does depend on Ω_0, albeit logarithmically, and increases as Ω_0 increases.

IV. LINE PROFILE

A. Linewidth

The expression for the transition probability (59), which in coherent atomic excitation represents the absorption line profile, allows us to derive an analytic formula for the absorption linewidth $\Delta_{1/2}$. The latter is defined as the detuning, for which the average (over $\sin^2$) transition probability $\overline{\mathcal{P}}(\Delta)$ decreases to one-half of its resonance value (half width at half maximum), $\overline{\mathcal{P}}(\Delta_{1/2}) = \frac{1}{2}\overline{\mathcal{P}}(0)$. With the observation that the transition probability (59) decreases with Δ mainly via the sech^2 factor, we find readily from Eq. (44) that

$$\Omega_0 = \frac{\Delta_{1/2}}{m} \exp\left[\frac{\pi}{4}\left(\zeta(\Delta_{1/2}T)^2 - \frac{1}{\zeta(\Delta_{1/2}T)^2}\right)\right], \tag{64}$$

where $\zeta = \pi/(2\,\mathrm{cosh}^{-1}\sqrt{2})^2 \approx 1.011\,043$

Equation (64) is qualitatively very similar to Eq. (16) derived from the adiabatic condition (13), except for the second (small) term in the exponent and small differences in the numeric factors.

Equation (64) gives the dependence of the peak Rabi frequency Ω_0 on the linewidth $\Delta_{1/2}$. It can be inverted (approximately) to provide the dependence of $\Delta_{1/2}$ on Ω_0. By taking logarithms of both sides of Eq. (64) and noting that Ω_0 grows exponentially with $\Delta_{1/2}$ (meaning that $\Omega_0 \gg \Delta_{1/2}$), we obtain

$$\Delta_{1/2} \approx \frac{2}{T\sqrt{\pi\zeta}} \sqrt{\ln(\Omega_0 T)}. \tag{65}$$

The latter equation shows that the linewidth is determined primarily by the pulse width T and increases only logarithmically with the Rabi frequency Ω_0. Hence there is a very weak, logarithmic power broadening, as demonstrated in Fig. 8.

Figure 9 shows a contour plot of the numerically calculated transition probability $\mathcal{P}$ for the Gaussian model (3) plotted versus the detuning Δ and the peak Rabi frequency Ω_0. As Ω_0 increases, Rabi-like oscillations appear along the vertical axis. In the horizontal direction $\mathcal{P}$ decreases as Δ increases away from resonance. The figure shows an excellent agreement of the analytically calculated linewidth (thick line) with the numerical results.

B. Comparison with other pulse shapes

The dependence (65) of the linewidth $\Delta_{1/2}$ on the Rabi frequency Ω_0 is different from those for other pulse shapes. For a rectangular pulse, the absorption line is Lorentzian and its width is proportional to Ω_0, indicating a typical power

broadening. For a hyperbolic-secant pulse, the line profile (63) is squared hyperbolic secant and its width does not depend on Ω_0 at all—i.e., there is no power broadenin—which is a unique feature for the sech pulse. Hence the Gaussian pulse is much closer to the hyperbolic secant but it is less adiabatic, which leads to weak, but nonzero power broadening.

V. CONCLUSIONS

In the present work we have derived analytically the transition probability between two quantum states driven by a pulsed field with a Gaussian temporal envelope. We have used the Dykhne-Davis-Pechukas method, which provides a very accurate approximation to the transition probability. We have derived both the amplitude and frequency of the Rabi-like oscillations induced by the Gaussian pulse. We have obtained an analytic formula for the width of the excitation line profile, which shows a weak, logarithmic power broadening.

ACKNOWLEDGMENTS

The authors acknowledge fruitful discussions with M. Fleischhauer. This work has been supported by the EU Research and Training Network COCOMO, Contract No. HPRN-CT-1999-00129. G.S.V. acknowledges support from EU Marie Curie Training Site Project No. HPMT-CT-2001-00294. N.V.V. acknowledges support from the Alexander von Humboldt Foundation.

APPENDIX: ASYMPTOTICS OF Im $\mathcal{D}(\tau_k^+)$ FOR LARGE α

In this appendix we derive the asymptotic behavior for $\alpha \gg 1$ of the imaginary part of the DDP integral $\mathcal{D}(\tau_k^+)$ for the kth transition point $\tau_k^+ = \xi_k + i\eta_k$. For large α, τ_k^+ has the asymptotic behavior (26), which implies that $\xi_k \gg 1 \gg \eta_k$; i.e., τ_k^+ is near the real axis. In order to calculate Im $\mathcal{D}(\tau_k^+)$ we choose an integration path, which initially follows the real axis from $\tau = 0$ to $\tau = \xi_k$ and then makes an upturn from $\tau = \xi_k$ to $\tau = \tau_k^+ = \xi_k + i\eta_k$. Since the real axis part gives only a real contribution to the integral, we have

$$\begin{aligned}
\mathrm{Im}\,\mathcal{D}(\tau_k^+) &= \Delta T\,\mathrm{Im}\int_{\xi_k}^{\xi_k + i\eta_k} \sqrt{\alpha^2 e^{-2\tau^2} + 1}\, d\tau \\
&= \Delta T \eta_k\,\mathrm{Re}\int_0^1 \sqrt{\alpha^2 e^{-2(\xi_k^2 - \eta_k^2 y^2) - 4i\xi_k\eta_k y} + 1}\, dy \\
&\sim \Delta T \eta_k\,\mathrm{Re}\int_0^1 \sqrt{\alpha^2 e^{-2\xi_k^2 - 4i\xi_k\eta_k y} + 1}\, dy \\
&= \Delta T \eta_k\,\mathrm{Re}\int_0^1 \sqrt{e^{-i(2k+1)\pi y} + 1}\, dy,
\end{aligned}$$

where we have changed the integration variable through $\tau = \xi_k + i\eta_k y$ and we have used the relations $\xi_k \gg 1 \gg \eta_k$, $e^{-2\xi_k^2} \sim \alpha^{-2}$ [see Eq. (26)], and $4\xi_k\eta_k = (2k+1)\pi$. By choosing a new integration variable $u = (2k+1)\pi y$ we find

$$\begin{aligned}
\mathrm{Im}\,\mathcal{D}(\tau_k^+) &\sim \frac{\Delta T \eta_k}{(2k+1)\pi}\,\mathrm{Re}\int_0^{(2k+1)\pi} \sqrt{1 + e^{-iu}}\, du \\
&= \frac{\Delta T \eta_k}{\pi}\,\mathrm{Re}\int_0^{\pi} \sqrt{1 + e^{-iu}}\, du,
\end{aligned}$$

because the integrand is a periodic function. Since $\mathrm{Re}\int_0^{\pi}\sqrt{1+e^{-iu}}\,du = \pi$, we obtain

$$\begin{aligned}
\mathrm{Im}\,\mathcal{D}(\tau_k^+) &\sim \Delta T \eta_k \sim \frac{(2k+1)\pi\Delta T}{4\sqrt{\ln\alpha}} \\
&\sim (2k+1)\,\mathrm{Im}\,\mathcal{D}(\tau_0^+) \quad (\alpha \gg 1). \qquad \text{(A1)}
\end{aligned}$$

[1] B. W. Shore, *The Theory of Coherent Atomic Excitation* (Wiley, New York, 1990).
[2] I. I. Rabi, Phys. Rev. **51**, 652 (1937).
[3] L. D. Landau, Phys. Z. Sowjetunion **2**, 46 (1932); C. Zener, Proc. R. Soc. London, Ser. A **137**, 696 (1932).
[4] N. Rosen and C. Zener, Phys. Rev. **40**, 502 (1932).
[5] L. Allen and J. H. Eberly, *Optical Resonance and Two-Level Atoms* (Dover, New York, 1987); F. T. Hioe, Phys. Rev. A **30**, 2100 (1984).
[6] A. Bambini and P. R. Berman, Phys. Rev. A **23**, 2496 (1981).
[7] Yu. N. Demkov and M. Kunike, Vestn. Leningr. Univ., Ser. 4: Fiz., Khim. **16**, 39 (1969); see also F. T. Hioe and C. E. Carroll, Phys. Rev. A **32**, 1541 (1985); J. Zakrzewski, *ibid.* **32**, 3748 (1985); K.-A. Suominen and B. M. Garraway, *ibid.* **45**, 374 (1992).
[8] Yu. N. Demkov, Sov. Phys. JETP **18**, 138 (1964).
[9] E. E. Nikitin, Opt. Spectrosc. **13**, 431 (1962); Discuss. Faraday Soc. **33**, 14 (1962); Adv. Quantum Chem. **5**, 135 (1970).
[10] A. M. Dykhne, Sov. Phys. JETP **11**, 411 (1960); **14**, 941 (1962).
[11] J. P. Davis and P. Pechukas, J. Chem. Phys. **64**, 3129 (1976).
[12] G. F. Thomas, Phys. Rev. A **27**, 2744 (1983).
[13] E. Bava, A. Godone, C. Novero, and H. O. Di Rocco, Phys. Rev. A **45**, 1967 (1992).
[14] P. R. Berman, L. Yan, K.-H. Chiam, and R. Sung, Phys. Rev. A **57**, 79 (1998).
[15] T. F. George and Y.-W. Lin, J. Chem. Phys. **60**, 2340 (1974).
[16] A. Joye, G. Mileti, and C.-E. Pfister, Phys. Rev. A **44**, 4280 (1991).
[17] K.-A. Suominen, B. M. Garraway, and S. Stenholm, Opt. Commun. **82**, 260 (1991).
[18] K.-A. Suominen and B. M. Garraway, Phys. Rev. A **45**, 374 (1992).
[19] K.-A. Suominen, Opt. Commun. **93**, 126 (1992).
[20] K.-A. Suominen, Ph.D. thesis, University of Helsinki, Finland, 1992.

[21] N. V. Vitanov and K.-A. Suominen, Phys. Rev. A **59**, 4580 (1999).

[22] M. Abramowitz and I. A. Stegun, *Handbook of Mathematical Functions* (Dover, New York, 1964).

[23] R. B. Dingle, *Asymptotic Expansions: Their Derivation and Interpretation* (Academic, London, 1973).

[24] D. S. F. Crothers, J. Phys. A **5**, 1680 (1972); J. Phys. B **6**, 1418 (1973).